Histogenesis of Clear Cell Adenocarcinoma in the Urinary Tract: Evidence of Urothelial Origin

Ming-Tse Sung,[1] Shaobo Zhang,[2] Gregory T. MacLennan,[4] Antonio Lopez-Beltran,[5] Rodolfo Montironi,[6] Mingsheng Wang,[2] Puay-Hoon Tan,[7] and Liang Cheng[2,3]

Abstract

Purpose: Clear cell adenocarcinoma in the urinary tract is a rare entity with an appearance resembling its counterpart in the female genital tract. Although several theories have been proposed about its origin, its exact histogenesis has remained uncertain.

Experimental Design: We integrated molecular genetic evaluation by fluorescence *in situ* hybridization and X-chromosome inactivation with conventional morphologic and immunohistochemical analyses in 12 patients with clear cell adenocarcinomas in the urinary tract.

Results: Concurrent urothelial carcinoma or urothelial carcinoma *in situ* was present in six cases (50%) and foci of cystitis glandularis were observed in four cases (33%). Neither intestinal metaplasia nor Müllerian component was identified in any case. Cytoplasmic expression of α-methylacyl-CoA racemase was demonstrable in 10 of 12 tumors (83%). Moderate to diffuse immunostaining for cytokeratin 7 was identified in all 12 tumors (100%), whereas only 3 of 12 (25%) tumors showed positive immunostaining for cytokeratin 20. Focal uroplakin III staining was seen in 6 of 12 tumors (50%). In five cases (42%), focal to moderate CD10 immunoreactivity was observed. Immunostains for OCT4 and CDX2 were completely negative in all tumors. In UroVysion fluorescence *in situ* hybridization assays, all tumors displayed chromosomal alterations similar to those commonly found in urothelial carcinoma. Identical patterns of nonrandom X-chromosome inactivation in concurrent clear cell adenocarcinoma and urothelial neoplasia were identified in two informative female cases.

Conclusions: Our findings support an urothelial origin for most clear cell adenocarcinomas of the urinary tract, despite their morphologic resemblance to certain Müllerian-derived tumors of the female genital tract.

Clear cell adenocarcinoma in the urinary tract is an extremely rare neoplasm predominantly occurring in adult females and morphologically identical to tumors of the same name that arise in female genital organs. Its precise histogenesis has remained controversial. It has been postulated to be of mesonephric origin (1), Müllerian origin (2–4), or urothelial origin (5, 6). The histogenetic connection between clear cell adenocarcinoma and adenocarcinoma of non-Müllerian type has been addressed by some investigators (6), and others have suggested that it results from malignant transformation of nephrogenic adenoma (7, 8). Previous investigations of its histogenesis have involved morphologic or immunohistochemical analyses of single cases or small series of cases. In our current study, we evaluated a large series of cases of clear cell adenocarcinoma of the urinary tract by molecular genetic appraisal with fluorescence *in situ* hybridization (FISH) and integrated these findings with conventional morphologic and immunohistochemical analyses in an effort to elucidate the histogenesis of this rare and enigmatic neoplasm.

Materials and Methods

Cases diagnosed as clear cell adenocarcinoma in the urinary tract were retrieved from the surgical pathology archives of the participating institutions. All slides were retrospectively reviewed and the diagnosis was confirmed in each case by reference to well-accepted diagnostic criteria (9). Twelve patients diagnosed between 1998 and 2006 whose tumors fulfilled the diagnostic criteria were selected for the current study. Clinical information was obtained from the medical records. The procedures applied in the current study were in accordance with institutional ethical standards.

Morphologic evaluation. Sections (4 μm thick) were cut from formalin-fixed and paraffin-embedded blocks and stained with H&E. All slides were evaluated for the structural patterns and cytologic features of clear cell adenocarcinoma. The tumor architecture was subclassified into three categories: tubulocystic, papillary, and solid

Authors' Affiliations: [1]Department of Pathology, Chang Gung Memorial Hospital-Kaohsiung Medical Center, Chang Gung University College of Medicine, Kaohsiung, Taiwan; [2]Departments of Pathology and Laboratory Medicine and [3]Urology, Indiana University School of Medicine, Indianapolis, Indiana; [4]Department of Pathology, Case Western Reserve University, Cleveland, Ohio; [5]Department of Pathology, Cordoba University, Cordoba, Spain; [6]Institute of Pathological Anatomy and Histopathology, School of Medicine, Polytechnic University of the Marche Region (Ancona), United Hospitals, Ancona, Italy; and [7]Department of Pathology, Singapore General Hospital, Singapore, Singapore

Received 9/10/07; revised 1/25/08; accepted 1/25/08.

The costs of publication of this article were defrayed in part by the payment of page charges. This article must therefore be hereby marked *advertisement* in accordance with 18 U.S.C. Section 1734 solely to indicate this fact.

Requests for reprints: Liang Cheng, Department of Pathology and Laboratory Medicine, Indiana University School of Medicine, 350 West 11th Street, Clarian Pathology Laboratory Room 4010, Indianapolis, IN 46202. Phone: 317-491-6442; Fax: 317-491-6419; E-mail: liang_cheng@yahoo.com.

doi:10.1158/1078-0432.CCR-07-4147

diffuse growth patterns. The tumor cells in all cases were evaluated for the presence or absence of clear cytoplasm, eosinophilic/basophilic cytoplasm, hobnail cell appearance, cellular pleomorphism, necrosis, and mitotic activity; the number of mitotic figures per 10 high-power fields in the most mitotically active areas was recorded in each case. The presence or absence of other associated pathologic findings that might be linked to tumor histogenesis, such as endometriosis, Müllerian remnants, cystitis glandularis, intestinal metaplasia, and accompanying urothelial neoplasia, was recorded.

Immunohistochemical analysis. Sections (4 μm thick) were cut for immunohistochemical staining, which was done on an automated immunostainer (DAKO). All slides were analyzed for immunoreactivity to the following antibodies: OCT4 (C20; 1:500 dilution; Santa Cruz Biotechnology), cytokeratin 7 (CK7; clone OV-TL 12/30; prediluted; DAKO), cytokeratin 20 (CK20; clone K_s20.8; prediluted; DAKO), CDX2 (clone CDX2-88; prediluted; Biogenex), CD10 (clone 56C3; prediluted; Cell Marque), uroplakin III (clone AU1; prediluted; Fitzgerald Industries International), and α-methylacyl-CoA racemase (AMACR; clone 13H4; 1:100 dilution; DAKO).

The slides were deparaffinized twice in xylene for 5 min and rehydrated through graded ethanol solutions to distilled water. Antigen retrieval was done by heating sections in 1 mmol/L EDTA (pH 8.0) for 30 min (OCT4), in citrate buffer for 15 min (CK20, CDX2, and uroplakin III), in alkali for 30 min (AMACR and CD10), or enzymatically with proteinase K (CK7). Inactivation of endogenous peroxidase activity was obtained by incubating sections in 3% H_2O_2 for 15 min. Protein block (DAKO) was applied for 20 min for blocking of nonspecific background staining. Bound antibodies were visualized with peroxidase-labeled streptavidin-biotin system (LSAB2 kit, DAKO) with 3,3′-diaminobenzidine as a chromogen. Appropriate positive controls for each antibody were run concurrently and showed adequate immunostaining.

Cytoplasmic staining for AMACR, membranous and cytoplasmic staining for CK7, CK20, uroplakin III, and CD10, and nuclear staining for OCT4 and CDX2 were assessed in a semiquantitative fashion in tumor cells. The percentages of positive tumor cells were estimated and the immunostaining results were categorized as negative (0%), focal (1-25%), moderate (26-50%), and diffuse (51-100%) as previously described (10 – 13).

Fluorescence* in situ *hybridization. From each specimen, multiple 4-μm unstained sections were prepared from buffered formalin-fixed, paraffin-embedded tissue blocks. A H&E-stained slide from each case was examined by pathologist to determine the area of interest. The unstained slides were deparaffinized with two changes of xylene, 15 min for each. Following the xylene, the slides were treated with two changes of absolute ethanol, 10 min each. The slides were air dried in the hood. Dried slides were boiled in a glass staining jar with 1× citrate buffer (pH 6.0; Zymed) within a beaker filled with distilled water on a hot block for 10 min. The boiled slides were kept in the citrate buffer until cooling down to the room temperature. The slides were removed from staining jar, washed with distilled water for 3 min, and then transferred to 2× SSC for 5 min. The slides were air dried and digested with 0.75 mL pepsin [5 mg/mL in 0.9% NaCl, 0.1 N HC1; Sigma Chemical Co.] at 37°C for 40 min. The slides were then washed with distilled water for 3 min and further washed with 2× SSC for 5 min and air dried. The CEP3 probe was labeled with Spectrum Red, CEP7 was labeled with Spectrum Green, LSI 9p21 was labeled with Spectrum Gold, and CEP17 was labeled with Spectrum Aqua (Vysis). The probes were diluted with *t*DenHyb2 (Insitus) in a ratio of 1:10. Diluted probes (5 μL) were added to the slide in the reduced light condition, the slide was covered with a 22 × 22 coverslip, and the edge was sealed with rubber cement. The slides were put into an opaque plastic box wrapped with aluminum foil. The slides were denatured at 83°C for 12 min and hybridized at 37°C overnight. After hybridization, the slides were washed at 45°C prewarmed 0.1× SSC with 1.5 mol/L urea twice, 20 min for each, following a wash with 2× SSC for 20 min and a 2× SSC/0.1% NP40 for 10 min at 45°C. The slides were further washed with 2× SSC for 5 min at room temperature. The slides were counterstained with 10 μL 4′,6-diamidino-2-phenylindole (DAPI; Insitus) for 2 min and covered with a 50 × 22 coverslip, and the edge was sealed with nail polish liquid.

The stained slides were observed and documented with a MetaSystem system under ×100 oil objective. The following filters were used: SP-100 for DAPI, FITC MF-101 for Spectrum Green, Gold 31003 for Spectrum Orange, Aqua 31036V2 for Spectrum Aqua, and TxRed Sp103 for Spectrum Red signals. Signals from each probe were counted under false color, with which the computer will show each color channels into red, green, gold, and aqua color. Five sequential focus stacks with 0.4-μm interval were acquired and then integrated into a single image to reduce thickness-related artifacts.

Two hundred cells were counted for each tissue specimen according to the H&E-stained slide. Typically, for normal cells, there were two signals from each probe in single diploid cells. Normal urothelial cells were used as negative controls and cutoff values were generated. Chromosomal gain or loss was defined based on the Gaussian model and relevant to the normal controls. The cutoff values were set at mean plus three SDs, which represent a specificity of 99.9%. Any tumor cases

Table 1. Clinicopathologic characteristics of 12 clear cell adenocarcinomas in the urinary tract

Characteristics	*n* (%)
Sex	
Male	4 (33)
Female	8 (67)
Age	Mean: 64 y (range, 41-75)
Tumor location	
Bladder	5 (42)
Urethra	7 (58)
Tumor size	Mean: 3.1 cm (range, 0.6-5.5)
Tumor architecture	
Tubulocystic	12 (100)
Papillary	7 (58)
Solid	5 (42)
Clear tumor cell	
Present	10 (83)
Absent	2 (17)
Hobnail cell	
Present	9 (75)
Absent	3 (25)
Eosinophilic/basophilic cytoplasm	
Present	12 (100)
Absent	0 (100)
Tumor cell pleomorphism	
Mild	0 (0)
Moderate	3 (25)
Severe	9 (75)
Tumor necrosis	
Present	8 (67)
Absent	4 (33)
Mitosis	Mean: 6 (range, 0-15)/ 10 high-power fields
Concurrent urothelial neoplasia	
Present	6 (50)
Absent	6 (50)
Endometriosis	
Present	0 (0)
Absent	12 (100)
Müllerian remnant	
Present	0 (0)
Absent	12 (100)
Cystitis glandularis	
Present	4 (33)
Absent	8 (67)
Intestinal metaplasia	
Present	0 (0)
Absent	100 (12)

Table 2. Staining results of various antibodies on immunohistochemistry in 12 clear cell adenocarcinomas in the urinary tract

Percentage of positive cells	Antibody, *n* (%)						
	AMACR	UroIII	OCT4	CK7	CK20	CD10	CDX2
0	2 (17)	6 (50)	12 (100)	0 (0)	9 (75)	7 (58)	12 (100)
1-25	3 (25)	6 (50)	0 (0)	1 (8)	0 (0)	3 (25)	0 (0)
26-50	4 (33)	0 (0)	0 (0)	2 (17)	2 (17)	2 (17)	0 (0)
51-100	3 (25)	0 (0)	0 (0)	9 (75)	1 (8)	0 (0)	0 (0)

Abbreviation: UroIII, uroplakin III.

with a score beyond the cutoff value were considered to have either a gain or a loss of the designated chromosomes.

X-chromosome inactivation analysis. X-chromosome inactivation analysis was done in tumor tissue from the female patients harboring clear cell adenocarcinoma and concurrent urothelial neoplasia. Histologic sections were prepared from formalin-fixed, paraffin-embedded blocks and stained with H&E for histologic examination and microdissection. Genomic DNA was prepared from both components of clear cell adenocarcinoma and urothelial neoplasia, microdissected by the PixCell II laser capture microdissection system (Arcturus), as previously described (14). Approximately 400 to 600 cells were microdissected from 5-μm histologic sections. Normal tissues microdissected from the same specimen were used as control samples for each patient.

The dissected cells were placed in 50 μL of buffer [i.e., 10 mmol/L Tris-HCl, 1 mmol/L EDTA, 1% Tween 20, 5 mg/mL proteinase K (pH 8.3)] and incubated overnight at 37°C. The solution was boiled for 10 min to inactivate the proteinase K and used directly for subsequent clonal analysis without further purification. Aliquots (8 μL) of the DNA extract were digested overnight at 37°C with 1 unit of *Hha*I restriction endonuclease (New England Biolabs, Inc.) in a total volume of 10 μL. Equivalent aliquots of the DNA extracts were also incubated in the digestion buffer without *Hha*I endonuclease as control reactions for each sample. After the incubation, 3 μL of digested or nondigested DNA were amplified in a 25-μL PCR volume containing 0.1 μL α-^{32}P–labeled dATP (3,000 Ci/mmol), 4 μmol/L androgen receptor (AR) sense primer (5′-TCCAGAATCTGTTCCAGAGCGTGC-3′), 4 μmol/L AR antisense primer (5′-GCTGTGAAGGTTGCTGTTCCTCAT-3′), 4% DMSO, 2.5 mmol/L $MgCl_2$, 300 μmol/L dCTP, 300 μmol/L dTTP, 300 μmol/L of each deoxynucleotide triphosphate, and 0.7 unit of Taq DNA polymerase (Perkin-Elmer Corp.). Each PCR amplification had an initial denaturation at 95°C for 8 min, followed by 38 cycles of 95°C for 40 s, 63°C for 40 s, and 72°C for 60 s, and then followed by a single final extension step at 72°C for 10 min. The PCR products were diluted with 4 μL of loading buffer containing 95% formamide, 20 mmol/L EDTA, 0.05% bromphenol blue, and 0.05% xylene cyanole FF (Sigma Chemical). The samples were heated to 95°C for 8 min and then chilled on ice. Three microliters of the reaction mixture were loaded onto 6.5% polyacrylamide denaturing gel and separated by electrophoresis at 1,600 V for 4 to 7 h. The bands were visualized after autoradiography with Kodak X-OMAT film (Eastman Kodak Company) for 8 to 16 h.

The clonality of the samples was evaluated based on a polymorphism of the X-linked *human AR* gene (*HUMARA*) locus (15). With this method, only the methylated *HUMARA* allele is amplified by PCR. The random inactive status of an X chromosome is established in all female somatic cells early in embryogenesis. The cases were considered to be informative if two AR allelic bands were detected after PCR amplification in normal control samples that had not been treated with *Hha*I. Only informative cases were included in the analysis. In tumor samples, nonrandom X-chromosome inactivation was defined as a complete or a nearly complete absence of an AR allele after *Hha*I digestion, which indicated a predominance methylation of one allele. Tumors were considered to be of the same clonal origin if the same AR allelic inactivation pattern was detected in both neoplasm components. Tumors were considered to be of independent origin if alternate predominance of AR alleles after *Hha*I digestion (different allelic inactivation patterns) was detected in the two components of the tumor.

Results

Clinical characteristics. The patient population consisted of four men and eight women with an age range of 41 to 75 years (mean, 65.2 years). Summaries of the clinicopathologic features, immunohistochemical characteristics, and UroVysion

Table 3. Chromosomal alterations detected by FISH UroVysion assay in 12 clear cell adenocarcinomas in the urinary tract

Case	Chromosome gain			Chromosome loss
	Chromosome 3	Chromosome 7	Chromosome 17	Chromosome 9p21
1	+	+	+	-
2	+	+	+	-
3	+	+	+	-
4	+	+	+	+
5	+	+	+	-
6	+	+	+	-
7	+	+	+	+
8	+	+	+	-
9	+	+	-	+
10	+	+	+	-
11	+	+	+	-
12	+	+	+	-

FISH assays are presented in Tables 1 to 3. Follow-up information was available in 11 patients. Mean follow-up was 29 months (range, 7-78 months). Seven of 11 cases remained alive during the follow-up period. Three patients were alive without evidence of residual disease at 24, 26, and 29 months after the initial diagnosis. Four patients died of cancer at 7, 13, 28, and 78 months after the first surgery and all of them developed metastatic lesions in various sites, including brain, lung, or pubic skin. One woman was alive 12 months after the diagnosis but had a local tumor recurrence. The remaining three patients ultimately developed retroperitoneal, pulmonary, or spinal metastases but all were still alive at 7, 8, and 58 months postoperatively.

Morphologic characteristics. Five clear cell adenocarcinomas arose in the urinary bladder and the remaining seven tumors were located in the urethra, one of which arose within a urethral diverticulum. All tumors were solitary, ranging from 0.6 to 5.5 cm (mean, 3.1 cm). The architectural patterns of tumor growth included tubulocystic, papillary, and solid diffuse patterns (Fig. 1). Two tumors exhibited exclusively tubulocystic architecture; the other 10 tumors were composed of more than one growth pattern and exhibited more complex architectural arrangements. Tubulocystic growth was the most common architectural pattern and was present in all 12 tumors (100%). Papillary and solid diffuse tumor architecture was observed in seven (58%) and five (42%) cases, respectively.

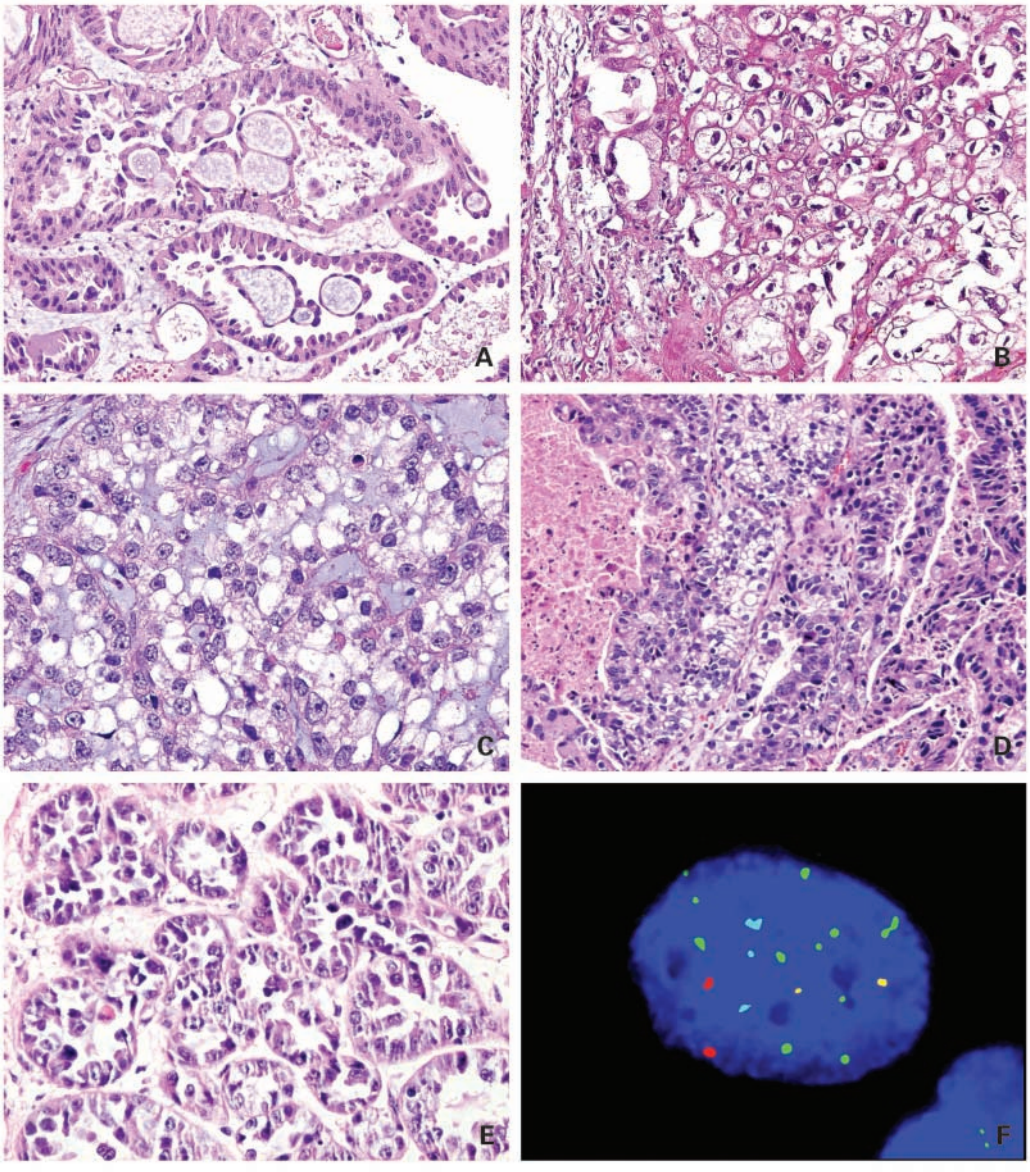

Fig. 1. Clear cell adenocarcinoma in the urinary tract. *A,* the tumor showed tubulocystic structure with characteristic lining hobnail cells. *B,* polygonal tumor cells revealed abundant clear cytoplasm. *C,* solid diffuse growth of clear cell adenocarcinoma, exhibiting marked cellular pleomorphism, nucleolar prominence, and mitotic activity. *D,* tumor necrosis was observed within the cystic space. The solid and tubular tumor components showed clear or eosinophilic cytoplasm. *E,* typical tubular formation with inner lining pleomorphic neoplastic cells. *F,* a typical tumor cell from clear cell adenocarcinoma of bladder showed chromosomal abnormalities detected by FISH. The cell showed gaining of chromosomes 7 (*green*) and 17 (*aqua*) but with normal copy numbers of chromosomes 3 (*red*) and 9p21 (*gold*).

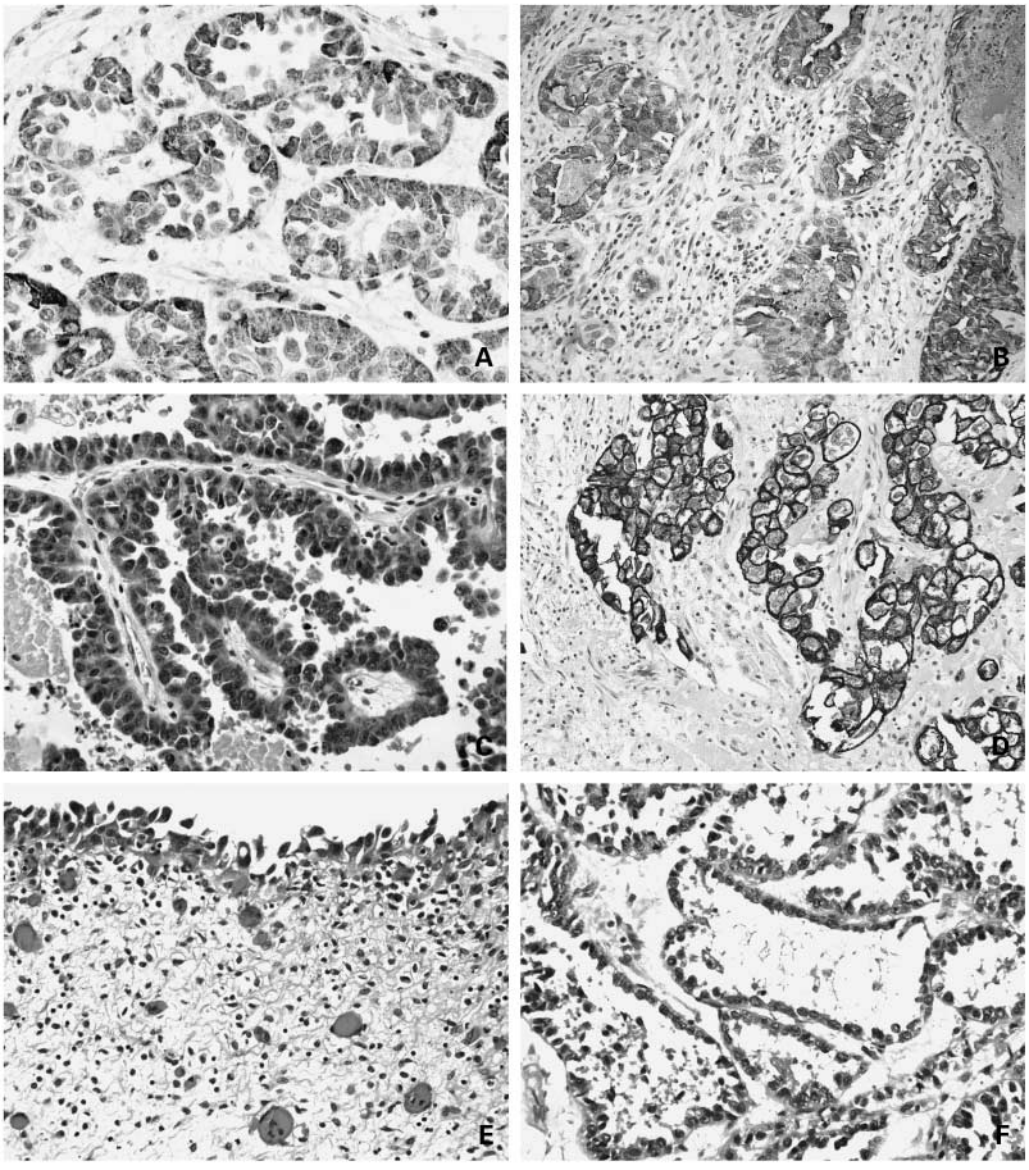

Fig. 2. Clear cell adenocarcinoma of the urinary tract. *A,* tumor cells were positively stained by AMACR, representing cytoplasmic staining in the tubular components. *B,* diffuse membranous and cytoplasmic expression of CD10. *C,* positive uroplakin III expression in clear cell adenocarcinoma. *D,* CK7 was strongly positive. *E* and *F,* a female patient represented with concurrent urothelial carcinoma *in situ* (*E*) and clear cell adenocarcinoma (*F*).

Tumor cells exhibited predominantly clear cytoplasm in 10 cases (83%), but in all cases, there were components of cells with eosinophilic or basophilic cytoplasm. Tumor cells lining tubules and cysts exhibited a "hobnail" appearance in nine tumors (75%). Nuclear pleomorphism of at least a moderate degree was evident in all tumors, and in nine cases, pronounced nuclear pleomorphism was observed. Tumor necrosis was a common finding, evident in eight cases (67%). The mean mitotic count was 6 (range, 0-15) per 10 high-power fields within the most mitotically active regions.

With regard to additional histologic findings that might have a bearing on tumor histogenesis, urothelial carcinoma or urothelial carcinoma *in situ* was present in six cases (50%), including four men and two women, and foci of cystitis glandularis were observed in four cases (33%). No case exhibited intestinal metaplasia or components of Müllerian derivation, such as endometriosis, endocervicosis, or endosalpingiosis.

Immunohistochemistry. Cytoplasmic expression of AMACR in tumor cells, with variable staining patterns, was observed in 10 of 12 tumors (83%; Fig. 2). Tumor cells in all cases showed positive immunostaining for CK7, which was typically moderate to strong and in diffuse staining patterns. In contrast, the majority of tumors showed negative immunostaining for CK20: only three (25%) tumors displayed significant expression in tumor cells. In five tumors (42%), membranous and cytoplasmic staining for CD10 was observed in <50% of tumor cells. Uroplakin III staining was identified in 6 of 12 tumors (50%), distributed in <25% of tumor cells. Immunostains for OCT4 and CDX2 were completely negative in all 12 clear cell adenocarcinomas in this study (Fig. 2).

Fluorescence **in situ** *hybridization.* All of the slides showed well-defined hybridization signals. UroVysion FISH assay displayed gains of both chromosomes 3 and 17 in all 12 tumors (100%), and gains of chromosome 7 in tumor cells were identified in 11 of 12 tumors (92%). In addition, loss of chromosome 9p21 was observed in three tumors (25%; Fig. 1).

X-chromosome inactivation analysis. The concurrent clear cell adenocarcinoma and urothelial neoplasia from two female patients were evaluated by X-chromosome inactivation analysis (Fig. 3). Both yielded informative results. Identical patterns of nonrandom inactivation of X-chromosome in components of clear cell adenocarcinoma and urothelial neoplasia were identified in both cases. This concordant pattern of X-chromosome inactivation in divergent tumor components indicates a common clonal origin for both clear cell adenocarcinoma and urothelial neoplasia.

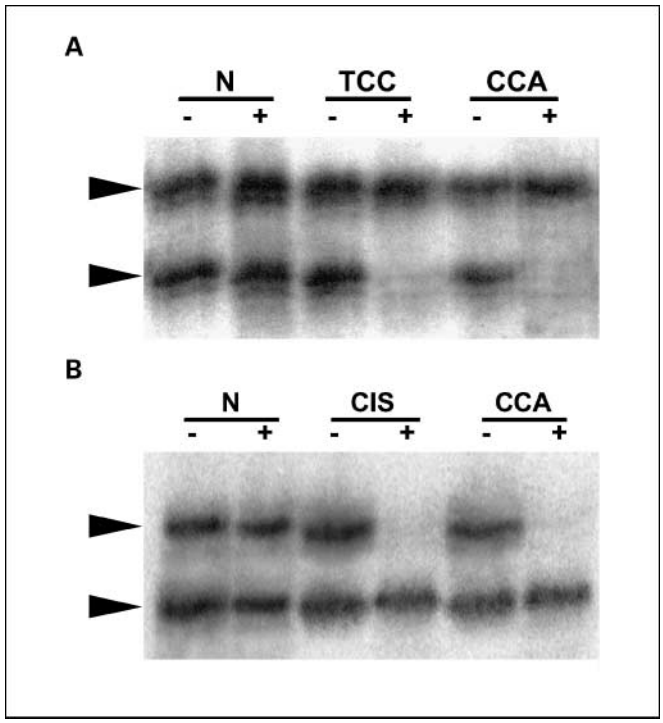

Fig. 3. Results of X-chromosome inactivation analysis in two female patients in whom clear cell adenocarcinoma coexisted with urothelial carcinoma (*A*) or urothelial carcinoma *in situ* (*B*). Concordant patterns of nonrandom inactivation of X-chromosome were identified in both components (clear cell adenocarcinoma and urothelial neoplasia) in both patients. Arrows, allelic bands. N, normal control tissue; TCC, urothelial (transitional cell) carcinoma component; CIS, urothelial carcinoma *in situ* component; CCA, clear cell adenocarcinoma component. -, without *Hha* I endonuclease digestion; +, after *Hha* I endonuclease digestion.

Discussion

In our current study investigating the histogenesis of clear cell adenocarcinomas of the urinary tract, we found that all tumors showed chromosomal alterations that are characteristically found in urothelial carcinoma, and extensive overlap between the immunoprofiles of clear cell adenocarcinoma and urothelial carcinoma. In addition, we noted a frequent association between clear cell adenocarcinoma and concurrent urothelial carcinoma, in which a common clonal origin of both tumor components was evident by identical nonrandom inactivation of X-chromosome and a notable absence of concurrent lesions of Müllerian derivation. Our findings support the hypothesis that most clear cell adenocarcinoma of the bladder and urethra arises from the urothelium.

The histogenesis of clear cell adenocarcinoma of the urinary tract has been a long-standing controversy. Attempts to clarify this issue using morphologic and immunohistochemical variables have produced conflicting results (Table 4). Clear cell adenocarcinoma was initially assumed to arise from the mesonephric duct vestiges or intermediate mesodermal vestiges near the vagina and was designated "mesonephric adenocarcinoma" based on this assumption (1), which had little scientific support (6, 16). The majority of clear cell adenocarcinomas in previous reports developed in females and resembled clear cell adenocarcinomas of Müllerian origin that arise in the female genital tract. Reports of coexistence of this neoplasm with vesical endometriosis, coupled with reports of immunoreactivity for CA-125, a putative marker for Müllerian differentiation (3, 4), were features initially favoring designation of the urinary tract neoplasm as "clear cell adenocarcinoma." Subsequent studies indicated a paucity of examples of coexisting clear cell adenocarcinoma and endometriosis, and furthermore, it became clear that CA-125 expression is not a specific marker for Müllerian differentiation (17). The hypothesis that clear cell adenocarcinoma is an adenocarcinoma of non-Müllerian origin is questionable because of the rarity of its association with intestinal metaplasia, a putative precursor of urinary tract adenocarcinoma (6). It has been proposed by some investigators that clear cell adenocarcinoma may be a malignant counterpart of nephrogenic adenoma (7, 8), a benign neoplasm characterized by proliferating tubules often lined by cells resembling hobnails. However, nephrogenic adenoma is much more common in males and does not share the typical topographical sites that characterize clear cell adenocarcinoma; furthermore, concurrence between the two entities is rare.

Divergent differentiation is a well-known characteristic of urothelial neoplasms, and for this reason, some investigators have proposed that clear cell adenocarcinoma arises from the urothelium and represents a particular morphologic variant with distinct glandular differentiation (5, 6, 18). In a study of 13 vesical clear cell adenocarcinomas, Oliva et al. (6) observed associated urothelial carcinoma or pseudostratified epithelium reminiscent of urothelium in nine tumors (69%) and proposed that these tumors were mostly of urothelial derivation.

It is widely believed that most human neoplasms, including tumors in the urinary bladder, result from a multistep process of accumulation of genetic alterations, such as the activation of oncogenes and/or loss of tumor suppressor genes (19). The inactivation of tumor suppressor genes by mutational events or by loss or replacement of chromosomal segments containing the critical tumor suppressor alleles provides selective advantages essential for progression or transformation of neoplasms. Therefore, an analysis of alterations of relevant chromosomes in tumor will provide invaluable information for elucidation of its pathogenesis. Recent advances in molecular genetics have indicated that urothelial carcinoma arises in a background of frequent alterations of a variety of chromosomes, such as chromosomes 3, 7, 9, and 17 (20, 21). Interphase FISH using fluorescent-labeled DNA probes to chromosomal centromeres or unique loci can be used to detect cells with these chromosomal alterations. A multicolor, multitarget interphase

FISH assay called UroVysion, consisting of probes to the centromeres of chromosomes 3, 7, and 17, and to the 9p21 region, has been recently shown to have high sensitivity and specificity for detecting urothelial carcinoma in urine specimens (22). We used this technology to show that clear cell adenocarcinomas of the urinary tract and urothelial carcinomas share multiple similar chromosomal changes. In contrast, the most frequent genetic alterations in ovarian clear cell adenocarcinomas occur on chromosome 1q (69%) (23). No genetic change is observed on chromosome 3 (0%) and only minimal genetic alterations occur on chromosome 7 (15%) and chromosome 17 (11%) (23). This profile of chromosomal abbreviations in ovarian clear cell adenocarcinoma is far different from that of clear cell adenocarcinoma of the urinary tract, in which gains of both chromosomes 3 and 17 were shown in all 12 tumors (100%) that we studied, and gains of chromosome 7 were identified in 11 of 12 tumors (92%). The marked disparity between the genetic profiles of clear cell adenocarcinoma of the urinary tract and those arising in the female genital tract strongly argues against the concept that these entities arise from a common histogenetic precursor.

The most consistently informative indicator of clonal origin of neoplasms in females is the nonrandom pattern of X-chromosome inactivation (24, 25). Neoplasia derived from a single progenitor cell is composed of cells in which the same X chromosome is inactivated. In our current study, the identical pattern of nonrandom X-chromosome inactivation between clear cell adenocarcinoma and concurrent urothelial neoplasia indicates that these morphologically diverse tumors are both derived from a common precursor cell; these data are additional support for the hypothesis that clear cell adenocarcinoma of the urinary tract is ultimately of urothelial cell origin.

Immunohistochemistry, in addition to its diagnostic applications, can also be helpful in understanding the nature and histogenesis of neoplasms. We assessed the immunoreactivity of urinary tract clear cell adenocarcinomas to several specific biomarkers and compared its immunoprofile with that of several possibly related lesions, specifically clear cell adenocarcinoma in female genital organs, nephrogenic adenoma, and urothelial carcinoma, in an attempt to ascertain any possible relationships between these entities.

OCT4 is a transcription factor that is fundamental in the maintenance of pluripotency in embryonic stem cells and in primordial germ cells and has recently been validated as a potent diagnostic utility for detecting specific types of germ cell tumors (11, 12). OCT4 expression by immunohistochemistry has also been reported in 28% of clear cell adenocarcinomas of the ovary (26). However, as noted, none of the urinary tract clear cell adenocarcinomas in our series showed positive immunostaining for OCT4.

CD10 is a cell surface metalloproteinase that is used for the diagnosis and grouping of leukemia/lymphoma. It is also expressed in several normal and neoplastic tissues (27–29), including urothelial carcinomas, which show mild to moderate CD10 staining in 43% of cases (27). It is notable that 41% of clear cell adenocarcinomas in our series similarly showed immunoreactivity to antibodies against CD10. In contrast, clear cell adenocarcinomas of Müllerian origin in the female

Table 4. Histogenetic theories of clear cell adenocarcinoma in the urinary tract (literature review of large-series studies and representative case reports)

Author	Publication year	Case number	Histogenetic origin	Methodology	Note
Konnak (1)	1973	1	Mesonephric	M	
Chor et al. (2)	1993	1	Müllerian	M	Associated endometriosis
Drew et al. (3)	1996	6	Müllerian	IHC	Positive for CA-125
Kunze (5)	1998	N/A	Urothelial	M	Transition of metaplastic urothelium into typical clear cell adenocarcinoma
Mai et al. (4)	2000	1	Müllerian	M	The presence of ciliated cells of Müllerian duct remnant
Oliva et al. (6)	2002	13	Urothelial	M	Nine tumors with concurrent urothelial carcinoma or epithelium reminiscent of urothelium were considered of urothelial origin. Four tumors associated with endometriosis or Müllerian remnant were of Müllerian origin
			Müllerian	IHC	
Suttmann et al. (8)	2006	1	Nephrogenic adenoma	M	Morphologic transition from nephrogenic adenoma to adenocarcinoma
Hartmann et al. (7)	2006	1	Nephrogenic adenoma	CGH	Similar genetic changes at chromosomes 4, 8, and 1 were found between nephrogenic adenoma and clear cell adenocarcinoma but different genomic alterations at chromosomes 9 and 17
Current study		12	Urothelial	M IHC FISH XCI	

Abbreviations: CGH, comparative genomic hybridization; IHC, immunohistochemistry; M, morphology; N/A, not available; XCI, X-chromosome inactivation.

genital tract were reportedly completely negative for CD10 expression (29).

The *CDX2* gene is a homeobox gene involved in regulating the differentiation and maintenance of intestinal epithelium (30). Several studies have shown significant expression of CDX2 in adenocarcinomas and intestinal metaplasia at various sites (31, 32). In the urinary tract, immunoreactivity to CDX2 has been reported in up to 83% of cases of intestinal metaplasia (13) and in 47% of primary adenocarcinomas (33), suggesting that intestinal differentiation is an inherent characteristic of most sporadic primary vesical adenocarcinomas. In contrast, it is notable that all of the urinary tract clear cell adenocarcinomas that we evaluated showed no immunoreactivity for this marker nor was there evidence of associated intestinal metaplasia in any of these cases, suggesting that intestinal differentiation is not an inherent feature of clear cell adenocarcinoma of the urinary tract.

AMACR/P504S, a 382–amino acid protein that plays an important role in bile acid synthesis and β-oxidation of branched chain fatty acid (34), has been validated as a useful auxiliary marker for the histologic diagnosis of prostate cancer (35, 36). However, AMACR expression is also demonstrable in a variety of normal tissues and malignant neoplasms (37) as well as in nephrogenic adenoma (38). There is some overlap between the histologic features of nephrogenic adenoma and those of clear cell adenocarcinoma, prompting the suggestion that nephrogenic adenoma might progress and transform into clear cell adenocarcinoma. We found similar rates of AMACR expression between clear cell adenocarcinoma in the current study and nephrogenic adenoma in the previous report (38). Although this may suggest a possible connection between these two entities, they have different CD10 expression profiles (39), markedly dissimilar gender predominance, and distinctly different topographical predilections. Hartmann et al. (7) described similar genetic changes at chromosomes 4, 8, and 1 in both lesions from a case with multiple recurrences of nephrogenic adenoma and ultimately the development of clear cell adenocarcinoma, but the fact that the two lesions in this patient had different genomic alterations at chromosomes 9 and 17 and the extremely limited case number in this report does not provide a firm evidence to support that these two lesions were causally related to one another. Considering that clear cell adenocarcinoma and urothelial neoplasia have similar expression profiles for AMACR (37) and CD10 (27), it seems reasonable to postulate that clear cell adenocarcinoma arises within urothelium.

CK7 is an intermediate filament that is found in urothelial neoplasia of the urinary bladder and serves as a sensitive marker for diagnosing urothelial carcinomas. In comparison, the incidence of positive expression of CK20 is relatively lower in urothelial neoplasia (40). In the current study, all clear cell adenocarcinomas showed moderate to diffuse CK7 expression, but only 25% of tumors exhibited CK20 staining. Our findings were similar to those noted by other investigators who evaluated 13 vesical clear cell adenocarcinomas and supported the notion of a probable histogenetic connection between clear cell adenocarcinoma and urothelial carcinoma (6).

Uroplakins, a group of transmembranous proteins constituting protein building blocks of the urothelial plaque, are products of terminally differentiated urothelium (41). Recently, uroplakin III has been validated as a highly specific immunohistochemical marker for urothelial neoplasms, although with only a moderate sensitivity (41–43). Kaufmann et al. (42) reported that 57% of urothelial carcinomas showed positive immunostaining for uroplakin III, but immunostaining for this marker in all other 318 nonurothelial carcinomas was consistently negative. In a microarray study, Parker et al. (43) observed a similar result, in which all 498 nonurothelial tumors and normal tissue were negative for uroplakin III immunoreactivity, but 64 of 112 (57%) urothelial tumors displayed uroplakin expression. In our current study, 6 of 12 (50%) clear cell adenocarcinomas showed uroplakin III immunoreactivity, an incidence entirely comparable with that observed in urothelial carcinoma. This pronounced similarity in degree of uroplakin III immunoreactivity in clear cell adenocarcinoma and urothelial carcinoma strongly supports the hypothesis that they share a close histogenetic origin, despite their morphologic dissimilarity.

In the morphologic analysis for the current series, clear cell adenocarcinomas comprised complex and mixed architectural growth pattern with easily identified cellular pleomorphism, frequent tumor necrosis, and appreciable mitotic activity. Characteristic clear tumor cell cytoplasm and hobnail tumor cells appeared in the majority of cases. All above histologic presentations were similar to the findings in the previous literatures (6, 16, 44, 45). In our study, neither Müllerian remnant, a clue of Müllerian origin as its genital counterpart, nor intestinal metaplasia, a common feature present in vesical adenocarcinoma of non-Müllerian origin, was identified. In contrast, half of the cases showed the concurrent urothelial carcinoma or urothelial carcinoma *in situ*, which strongly implicated the close relationship between clear cell adenocarcinoma and urothelial carcinoma.

In summary, clear cell adenocarcinomas of the urinary tract frequently coexist with urothelial neoplasia, have an immunoprofile that significantly overlaps with that of urothelial carcinoma, exhibit genetic aberrations that are identical to those commonly observed in urothelial carcinoma, and share a common clonal origin with concurrent urothelial carcinoma. These findings strongly support an urothelial origin for most clear cell adenocarcinomas of the urinary tract, despite their morphologic resemblance to tumors commonly found in the female genital tract.

References

1. Konnak JW. Mesonephric carcinoma involving the urethra. J Urol 1973;110:76–8.
2. Chor PJ, Gaum LD, Young RH. Clear cell adenocarcinoma of the urinary bladder: report of a case of probable mullerian origin. Mod Pathol 1993;6:225–8.
3. Drew P, Murphy WM, Civantos F, et al. The histogenesis of clear cell adenocarcinoma of the lower urinary tract: case series and review of the literature. Hum Pathol 1996;27:248–52.
4. Mai KT, Yazdi HM, Perkins DG, et al. Multicentric clear cell adenocarcinoma in the urinary bladder and the urethral diverticulum: evidence of origin of clear cell adenocarcinoma of the female lower urinary tract from Mullerian duct remnants. Histopathology 2000;36:380–2.
5. Kunze E. Histogenesis of nonurothelial carcinomas in the human and rat urinary bladder. Exp Toxicol Pathol 1998;50:341–55.
6. Oliva E, Amin MB, Jimenez R, et al. Clear cell carcinoma of the urinary bladder: a report and comparison of four tumors of mullerian origin and nine of probable urothelial origin with discussion of histogenesis and diagnostic problems. Am J Surg Pathol 2002;26:190–7.

7. Hartmann A, Junker K, Dietmaier W, et al. Molecular evidence for progression of nephrogenic metaplasia of the urinary bladder to clear cell adenocarcinoma. Hum Pathol 2006;37:117–20.

8. Suttmann H, Holl-Ulrich K, Peter M, et al. Mesonephroid adenocarcinoma arising from mesonephroid metaplasia of the urinary bladder. Urology 2006;67: 846.e7–8.

9. Eble JN, Sauter G, Epstein JI, et al. World Health Organization classification of tumours: pathology and genetics of tumours of the urinary system and male genital organs. Lyon: IARC Press; 2004.

10. Sung MT, Jiang Z, Montironi R, et al. α-Methylacyl-CoA racemase P504S/34βE12/p63 triple cocktail stain in prostatic adenocarcinoma after hormonal therapy. Hum Pathol 2007;38:332–41.

11. Sung MT, JonesTD, Beck SD, et al. OCT4 is superior to CD30 in the diagnosis of metastatic embryonal carcinomas after chemotherapy. Hum Pathol 2006;37: 662–7.

12. Cheng L. Establishing a germ cell origin for metastatic tumors using OCT4 immunohistochemistry. Cancer 2004;101:2006–10.

13. Sung MT, Lopez-Beltran A, Eble JN, et al. Divergent pathway of intestinal metaplasia and cystitis glandularis of the urinary bladder. Mod Pathol 2006; 19:1395–401.

14. Sung MT, Wang M, Maclennan G, et al. Histogenesis of sarcomatoid urothelial carcinoma of the urinary bladder: evidence for a common clonal origin with divergent differentiation. J Pathol 2007;211:420–430.

15. Mashal RD, Lester SC, Sklar J. Clonal analysis by study of X chromosome inactivation in formalin-fixed paraffin-embedded tissue. Cancer Res 1993;53: 4676–79.

16. Young RH, Scully RE. Clear cell adenocarcinoma of the bladder and urethra. A report of three cases and review of the literature. Am J Surg Pathol 1985;9: 816–26.

17. Torenbeek R, Lagendijk JH, van Diest PJ, et al. Value of a panel of antibodies to identify the primary origin of adenocarcinomas presenting as bladder carcinoma. Histopathology 1998;32:20–7.

18. Gilcrease MZ, Delgado R, Vuitch F, et al. Clear cell adenocarcinoma and nephrogenic adenoma of the urethra and urinary bladder: a histopathologic and immunohistochemical comparison. Hum Pathol 1998; 29:1451–6.

19. Takahashi T, Habuchi T, Kakehi Y, et al. Clonal and chronological genetic analysis of multifocal cancers of the bladder and upper urinary tract. Cancer Res 1998;58:5835–41.

20. Orntoft TF, Wolf H. Molecular alterations in bladder cancer. Urol Res 1998;26:223–33.

21. Sandberg AA, Berger CS. Review of chromosome studies in urological tumors. II. Cytogenetics and molecular genetics of bladder cancer. J Urol 1994;151: 545–60.

22. Skacel M, Fahmy M, Brainard JA, et al. Multitarget fluorescence *in situ* hybridization assay detects transitional cell carcinoma in the majority of patients with bladder cancer and atypical or negative urine cytology. J Urol 2003;169:2101–5.

23. Okada S, Tsuda H, Takarabe T, et al. Allelotype analysis of common epithelial ovarian cancers with special reference to comparison between clear cell adenocarcinoma with other histological types. Jpn J Cancer Res 2002;93:798–806.

24. Cheng L, Jones TD, McCarthy RP, et al. Molecular genetic evidence for a common clonal origin of urinary bladder small cell carcinoma and coexisting urothelial carcinoma. Am J Pathol 2005;166:1533–9.

25. Cheng L, Gu J, Eble JN, et al. Molecular genetic evidence for different clonal origin of components of human renal angiomyolipoma. Am J Surg Pathol 2001;25:1231–6.

26. Cheng L, Thomas A, Roth LM, et al. OCT4: a novel biomarker for dysgerminoma of the ovary. Am J Surg Pathol 2004;28:1341–6.

27. Bircan S, Candir O, Kapucuoglu N, et al. CD10 expression in urothelial bladder carcinomas: a pilot study. Urol Int 2006;77:107–13.

28. Chu PG, Arber DA, Weiss LM, et al. Utility of CD10 in distinguishing between endometrial stromal sarcoma and uterine smooth muscle tumors: an immunohistochemical comparison of 34 cases. Mod Pathol 2001;14:465–71.

29. Ordi J, Romagosa C, Tavassoli FA, et al. CD10 expression in epithelial tissues and tumors of the gynecologic tract: a useful marker in the diagnosis of mesonephric, trophoblastic, and clear cell tumors. Am J Surg Pathol 2003;27:178–86.

30. Silberg DG, Sullivan J, Kang E, et al. Cdx2 ectopic expression induces gastric intestinal metaplasia in transgenic mice. Gastroenterology 2002;122: 689–96.

31. Ko S, Chu KM, Luk JM, et al. CDX2 co-localizes with liver-intestine cadherin in intestinal metaplasia and adenocarcinoma of the stomach. J Pathol 2005; 205:615–22.

32. Osawa H, Kita H, Satoh K, et al. Aberrant expression of CDX2 in the metaplastic epithelium and inflammatory mucosa of the gallbladder. Am J Surg Pathol 2004;28:1253–4.

33. Suh N, Yang XJ, Tretiakova MS, et al. Value of CDX2, villin, and α-methylacyl coenzyme A racemase immunostains in the distinction between primary adenocarcinoma of the bladder and secondary colorectal adenocarcinoma. Mod Pathol 2005;18: 1217–22.

34. Ferdinandusse S, Denis S, L IJ, et al. Subcellular localization and physiological role of α-methylacyl-CoA racemase. J Lipid Res 2000;41:1890–6.

35. Luo J, Zha S, Gage WR, et al. α-Methylacyl-CoA racemase: a new molecular marker for prostate cancer. Cancer Res 2002;62:2220–6.

36. Rubin MA, Zhou M, Dhanasekaran SM, et al. α-Methylacyl coenzyme A racemase as a tissue biomarker for prostate cancer. JAMA 2002;287: 1662–70.

37. Jiang Z, Fanger GR, Woda BA, et al. Expression of α-methylacyl-CoA racemase P504s in various malignant neoplasms and normal tissues: a study of 761 cases. Hum Pathol 2003;34:792–6.

38. Skinnider BF, Oliva E, Young RH, et al. Expression of α-methylacyl-CoA racemase P504S in nephrogenic adenoma: a significant immunohistochemical pitfall compounding the differential diagnosis with prostatic adenocarcinoma. Am J Surg Pathol 2004;28:701–5.

39. Xiao GQ, Burstein DE, Miller LK, et al. Nephrogenic adenoma: immunohistochemical evaluation for its etiology and differentiation from prostatic adenocarcinoma. Arch Pathol Lab Med 2006;130:805–10.

40. Jiang J, Ulbright TM, Younger C, et al. Cytokeratin 7 and cytokeratin 20 in primary urinary bladder carcinoma and matched lymph node metastasis. Arch Pathol Lab Med 2001;125:921–3.

41. Moll R, Wu XR, Lin JH, et al. Uroplakins, specific membrane proteins of urothelial umbrella cells, as histological markers of metastatic transitional cell carcinomas. Am J Pathol 1995;147:1383–97.

42. Kaufmann O, Volmerig J, Dietel M. Uroplakin III is a highly specific and moderately sensitive immunohistochemical marker for primary and metastatic urothelial carcinomas. Am J Clin Pathol 2000;113:683–7.

43. Parker DC, Folpe AL, Bell J, et al. Potential utility of uroplakin III, thrombomodulin, high molecular weight cytokeratin, and cytokeratin 20 in noninvasive, invasive, and metastatic urothelial (transitional cell) carcinomas. Am J Surg Pathol 2003;27:1–10.

44. Meis JM, Ayala AG, Johnson DE. Adenocarcinoma of the urethra in women. A clinicopathologic study. Cancer 1987;60:1038–52.

45. Oliva E, Young RH. Clear cell adenocarcinoma of the urethra: a clinicopathologic analysis of 19 cases. Mod Pathol 1996;9:513–20.